

Explaining Domain Shifts in Language: Concept erasing for Interpretable Image Classification

Zequn Zeng^{1*}, Yudi Su^{1*}, Jianqiao Sun¹, Tiansheng Wen¹,

Hao Zhang¹, Zhengjue Wang², Bo Chen^{1†}, Hongwei Liu^{1†} and Jiawei Ma³

¹National Key Laboratory of Radar Signal Processing, Xidian University, Xi’an, 710071, China.

²State Key Laboratory of Integrated Service Networks, Xidian University, Xi’an, 710071, China.

³City University of Hong Kong, Hong Kong SAR.

zqzeng-1@stu.xidian.edu.cn, bchen@mail.xidian.edu.cn

Abstract

Concept-based models can map black-box representations to human-understandable concepts, which makes the decision-making process more transparent and then allows users to understand the reason behind predictions. However, domain-specific concepts often impact the final predictions, which subsequently undermine the model generalization capabilities, and prevent the model from being used in high-stake applications. In this paper, we propose a novel **Language-guided Concept-Erasing (LanCE)** framework. In particular, we empirically demonstrate that pre-trained vision-language models (VLMs) can approximate distinct visual domain shifts via domain descriptors while prompting large Language Models (LLMs) can easily simulate a wide range of descriptors of unseen visual domains. Then, we introduce a novel plug-in domain descriptor orthogonality (DDO) regularizer to mitigate the impact of these domain-specific concepts on the final predictions. Notably, the DDO regularizer is agnostic to the design of concept-based models and we integrate it into several prevailing models. Through evaluation of domain generalization on four standard benchmarks and three newly introduced benchmarks, we demonstrate that DDO can significantly improve the out-of-distribution (OOD) generalization over the previous state-of-the-art concept-based models. Our code is available at <https://github.com/joeyz0z/LanCE>.

1. Introduction

Concept-based models [11, 27, 42] are prominent approaches for achieving model interpretability, which leverage human-understandable concepts to explain the black-box image representation. Specifically, these models first

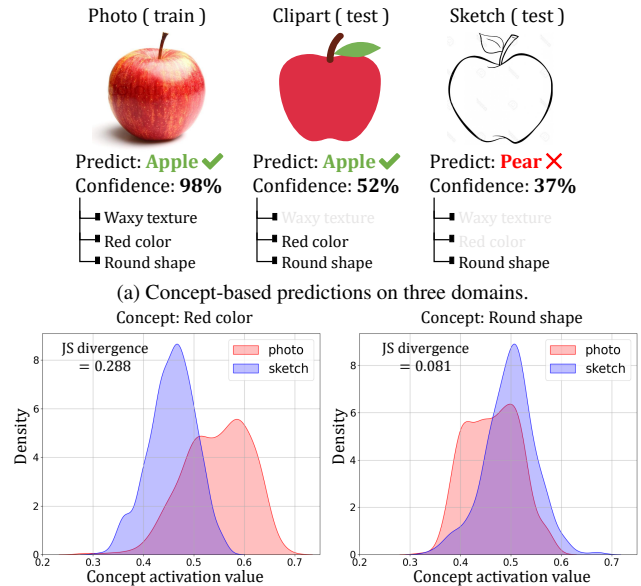


Figure 1. Domain shifts in concept space. (a) Given the images of an apple in different visual domains, the prediction confidence of a concept-based model, trained on the photo domain, degrades due to the missing of concepts. (b) Distribution comparison of concept activation value (image-concept similarity computed via CLIP [26]) between photo domain and sketch domain, for two concepts, *i.e.*, “red color” and “round shape”, respectively. JS divergence indicates the distance between two distributions and tends to be larger for domain-specific concepts (*e.g.* “red color”).

map the image feature to a concept activation vector in a concept space (each dimension corresponds to an interpretable concept) and then use the concept activation vector to predict the final output. Recently, equipped with pre-trained vision-language models (VLMs) [8, 26], concept-based models [41, 42] can obtain the concept activation value by calculating the similarity between image embed-

*Equal contribution. †Corresponding authors

dings and textual concept embeddings.

Nevertheless, current concept-based models still struggle to handle domain shifts encountered during inference. The distinct distribution of visual concepts across different domains presents a significant generalization challenge for these models. As shown in Fig. 1a, the concept-based models trained on the photographic images usually excel at associating the discriminative visual clues – such as red color, waxy texture, and round shape – with specific classes like “apple”, akin to human beings. However, these models experience substantial performance degradation when applied to images in unseen visual domains, such as clipart or sketches, due to the absence of domain-specific texture and color concepts. These domain-specific concepts (*e.g.* “red color”) generally exhibit a larger distributional difference between visual domains than domain-shared concepts (*e.g.* “round shape”), as illustrated in Fig. 1b. Consequently, the concept-based models trained on a single domain are inevitably biased to associate those domain-specific concepts with the final predictions, thereby limiting their out-of-distribution (OOD) generalization capabilities.

To mitigate the issue of domain shifts in the concept space, a straightforward solution is to involve human experts in filtering out the domain-specific concepts and retaining only domain-shared concepts for classification tasks, which is nevertheless labor-intensive. Another possible solution is to diversify the training domain [1, 3] to mitigate the impact of the domain-specific concepts. However, it is impractical to cover all possible unseen domains during training exhaustively. Additionally, current domain generalization approaches [49] can not be directly applied to concept-based models due to the lack of interpretability of semantics of the learned representation [34]. Therefore, automating the identification and elimination of domain-specific concepts remains an under-explored area.

In this paper, we propose a **Language-guided Concept-Erasing** framework, namely **LanCE**, to enhance the OOD generalization capabilities of current concept-based models. Specifically, we empirically demonstrate that pre-trained VLMs, such as CLIP, can interpret the domain shifts through language, *i.e.*, domain shifts can be approximated by a set of domain descriptors generated by large language models (LLMs). To alleviate the biased association between final predictions and domain-specific concepts, we introduce a plug-in domain descriptor orthogonality (DDO) loss that reduces the fluctuation of concept activation caused by these language-guided domain shifts. We evaluate our method on seven benchmarks, including four common benchmarks (CUB-Painting [35], PACS [13], Office-Home [31] and DomainNet [24]), and three new proposed benchmarks (Awa2-clipart, LADA-Sculpture and LADV-3D) based on several existing visual classification datasets with concept annotations [39, 47]. These newly-collected

datasets are gathered from the web and manually filtered. Extensive experiments demonstrate that the proposed approach can preserve the In-distribution (ID) classification capabilities and significantly improve the OOD generalization capabilities of prevailing concept-based models. Our contributions can be summarized as follows:

- We provide a concept-level explanation for the domain shifts and empirically reveal that VLMs can represent visual domain shifts into language space.
- Based on this observation, we propose a plug-in domain descriptor orthogonality regularizer to learn a domain-shared concept-based model without changing the model architecture and increasing training data.
- We introduce three new concept-based OOD generalization benchmarks including more challenging scenarios such as natural photos→3D-renders and real animals→sculptures. Extensive experiments on four common and three new benchmarks demonstrate that our proposed method significantly improves the OOD generalization capabilities of current concept-based models.

2. Related Work

Concept-based models are one of the mainstream interpretable approaches that aim to understand models by associating black box features with meaningful concepts. Current concept-based models can broadly be divided into two categories, concept bottleneck models (CBMs) [11] which map the image features into an intermediate concept bottleneck layer whose neurons indicate concept activation values of pre-defined concepts, and concept activation vectors (CAVs) [9] which represent concepts as normal vectors of decision boundaries that distinguish positive and negative samples of a concept. Vanilla CBM requires fine-grained and precise concept annotation on the concept bottleneck layer and CAVs need positive and negative samples of each concept to learn meaningful concept representations. Many recent approaches are proposed to tackle the above concerns from two perspectives. On the one hand, many methods generate the concepts derived from ConceptNet [42], LLMs [21, 41] or multimodal datasets [28, 43] to automate the construction of the concept bottleneck layer. On the other hand, to remove the reliance on human-annotated concept labels, these methods deploy pre-trained VLMs such as CLIP to map concepts to text embeddings and compute image-concept similarity to serve as concept activation annotations. However, concepts of the above approaches are typically domain-sensitive and the corresponding concept activations have large distributional differences across various domains. They often fail to handle domain shifts when applied to unseen domains.

Domain adaptation & generalization aims to handle the domain shifts between training and test data. In contrast to traditional deep learning based on in-distribution assump-

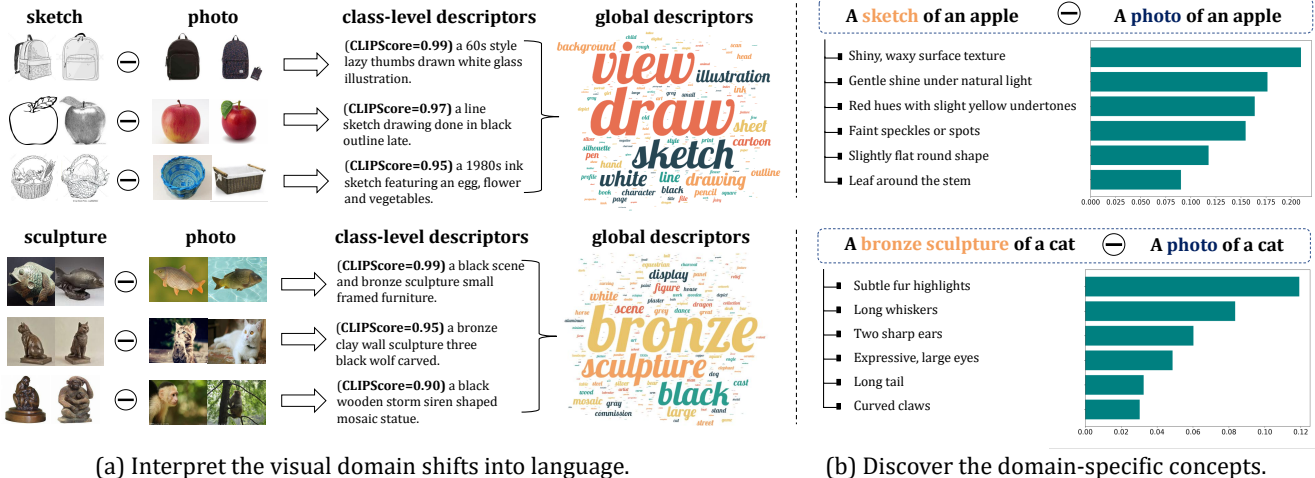


Figure 2. (a) We empirically demonstrate that the visual domain shift can be interpreted in language. For each class, we obtain the caption from the embedding difference of images from two domains. Then, by aggregating the captions across the classes, the keywords regarding the domain shift can be highlighted. At the same time, (b) the domain-specific concepts can be discovered from language descriptions of the different domains. In detail, they have higher similarities with the difference of domain-related class descriptions, *i.e.*, textural domain shift, in the CLIP embedding space. More analyses are shown in the Appendix B.

tion, domain adaptation methods [4, 20] target to improve the performance on the target domain when only a few samples [14] or unlabeled data [40] from target domains are available. Instead, domain generalization methods [49] focused on more difficult scenarios in which no target domain data are available during the training phase. The setting of this paper belongs to the single domain generalization scenario, *i.e.* only one single domain is available during training [19, 36, 48]. While the domain generalization area is well studied, there is still researcher doubt about the interpretability of domain generalization methods [34]. Although disentanglement-based domain generalization methods [25, 33] decompose a feature into domain-shared and domain-specific parts, there is still a lack of deep understanding of the semantics of the learned features in domain generalization models. Our proposed method provides a concept-level explanation of domain shifts and takes steps to interpretable domain generation.

Vision-Language Pretraining aims to bridge the gap between image and text representations. Compared with vision-only pretraining methods [5, 6, 17], vision-language pertaining like CLIP [26] achieved remarkable success and showed superior performance on some high-level vision understanding tasks [16, 44, 46] and multi-modality tasks [29, 38, 45]. Our empirical findings further validate that CLIP can interpret a variety of domain shifts into a set of domain descriptors.

3. Empirical Observations

This section demonstrates that the pre-trained VLMs can approximate the visual domain shifts via domain descrip-

tors. Meanwhile, these language-guided domain shifts can effectively distinguish the domain-specific concepts as illustrated in Fig. 2. It serves as the key insight for our proposed LanCE method.

Image-text alignment. CLIP trained on multi-modal contrastive learning, can effectively bridge the gap between image representation and text representation. The alignment facilitates a new approach to manipulate images using language, applicable for various vision tasks, *e.g.* image editing [7, 23], style transfer [12, 37], data augmentation [2, 3, 18]. The CLIP image-text similarity can be computed as:

$$\mathcal{L}_{\text{CLIP}}(I, T) = \text{sim}(E_I(I), E_T(T)) \quad (1)$$

where E_I and E_T mean the image encoder and text encoder of CLIP, respectively. sim indicate the cosine similarity.

Interpreting the visual domain shifts. Inspired by previous works [2, 23], we assume that the visual domain shifts and descriptions of domain changes are aligned within the CLIP embedding space. To validate this hypothesis, we employ a CLIP-based zero-shot captioner [44] to translate the visual embedding differences into language, as illustrated in Fig. 2(a). Let $\{I_c^{\text{src}}\}$ and $\{I_c^{\text{tgt}}\}$ denote the images of the same class c from the source domain and the target domain, respectively. The class-level visual domain gap Δd_c and corresponding description t_c can be generated by solving the following maximization problem:

$$\max_{t_c} \mathcal{L}_{\text{CLIP}}(\Delta d_c, t_c), \quad (2)$$

$$\Delta d_c = \mathbb{E}(E_I(I_c^{\text{tgt}})) - \mathbb{E}(E_I(I_c^{\text{src}})), \quad (3)$$

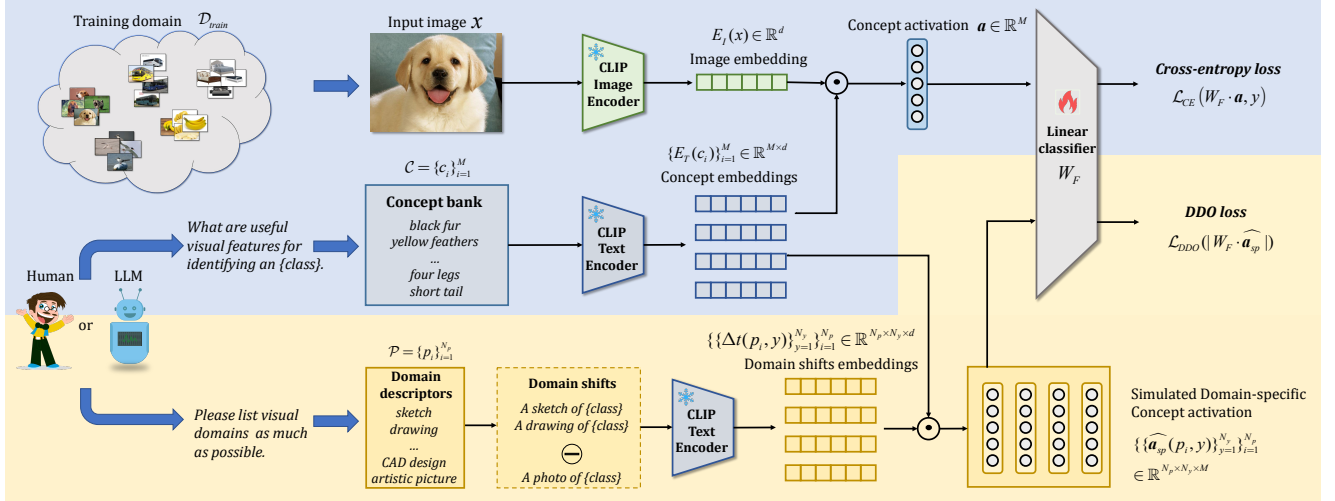


Figure 3. Overview of the LanCE. **Blue part** is the data flow of vanilla CLIP-CBMs (Sec. 4.1). To provide concept-level explanations, we first construct a human-written or LLMs-generated concept set \mathcal{C} and extract the concept embeddings via the frozen CLIP text encoder. Given an image, we can extract the image embeddings via the frozen CLIP image encoder. The concept activations are the cosine similarity between image embeddings and concept embeddings. A learnable linear layer W_F is fitted on top of the concept activation vector and is responsible for predicting the final class and is optimized via cross-entropy loss. **Yellow part** is the data flow of our proposed DDO regularizer (Sec. 4.2). Similarly, we first construct a domain descriptor set (Sec. 4.3) to obtain the language-guided domain shifts and then simulate the domain-specific concept activations. To erase the effect of domain-specific concepts, the DDO regularizer encourages the orthogonality between the class-concept correlation matrix W_F (*i.e.* the final linear weight) and domain-specific concept activation $\widehat{\mathbf{a}}_{sp}$.

As shown in Fig. 2(a), we produce high-matching (CLIP-Score > 0.9) descriptions t_c that effectively interpret the class-level visual domain gap Δd_c between sketch images, sculpture images and photographic images. We observe that these class-level domain descriptors are typically descriptions of the style difference of the two domains, regarding class-level domain descriptors. To further get the global difference between the two domains, we aggregate all class-level domain descriptors and transfer them into word cloud format, where the word size is proportional to the word frequency in the generated domain description corpus. As a result, we empirically find that global visual domain descriptors Δd primarily consist of style words such as “sketch and sculpture” and background words *e.g.* “white”.

Discover the domain-specific concepts. Since we have revealed that visual domain shifts and descriptions of domain changes are aligned within the CLIP embedding space, we can synthesize the visual domain shifts via domain descriptors. Subsequently, we can leverage these language-guided domain shifts to discover domain-specific concepts. Specifically, we compute the similarity between textual domain shift embeddings (*e.g.* “A sketch of an apple” - “A photo of an apple”) and all candidate concept embeddings extracted by CLIP text encoder. The results in Fig. 2(b) show that domain-specific concepts like “shiny, waxy surface texture” generally exhibit a higher similarity score due to their substantial distribution shift between those two domains while those domain-shared concepts such as “Leaf around

the stem” have relatively lower similarity score. Consequently, we can distinguish the domain-specific concepts via language-guided domain shifts.

4. Method

To improve the generalization capabilities of prevailing concept-based models, as shown in Fig. 3, we propose a novel **LanCE** framework. In this section, we first formulate the problem and introduce Concept bottleneck models (CBMs), which can effectively map the black-box visual features to human-understandable concept space to interpret the final outputs (Sec. 4.1). However, domain-specific concepts will undermine the generalization capabilities. Then, to alleviate the biased association between domain-specific concepts and class predictions within the learnable linear classifier, we propose a domain descriptor orthogonality loss to improve the OOD classification performances of concept-based models (Sec. 4.2). Furthermore, considering all possible visual domains, we prompt LLMs to generate a bunch of domain descriptors to simulate numerous unseen visual domains (Sec. 4.3).

4.1. Problem Formulation

Given a training domain data $\mathcal{D}_{train} = \{(x_i, y_i)\}$, where $x_i \in \mathcal{X}$ are training images and $y_i \in \mathcal{Y}$ are corresponding labels, the concept-based models are trained only on \mathcal{D}_{train} , however evaluated on both \mathcal{D}_{train} and k unseen domains

$\{\mathcal{D}_{unseen}^i\}_{i=1}^k$. To provide a concept-level explanation, we should construct a concept set $\mathcal{C} = \{c_i\}_{i=1}^M$ including M interpretable concepts written by humans or LLMs. To evaluate the effectiveness of our method, we choose the well-studied concept bottleneck models (CBMs) family as the baselines of our methods. As one of the main branches of concept-based models, CBMs first project the image feature to an intermediate concept bottleneck layer to obtain the concept activation vector. Each activation value indicates the presence of the corresponding concept in the input. The forward pipeline of vanilla CBM [11] can be formulated as:

$$\mathbf{a} = f_C(f_I(\mathbf{x})), \quad (4)$$

$$\hat{y} = f_F(\mathbf{a}) = W_F \cdot \mathbf{a}, \quad (5)$$

where $\mathbf{a} \in \mathbb{R}^M$ is the concept activation vector, $f_I : \mathbb{R}^{h \times w} \rightarrow \mathbb{R}^d$ is the image feature extractor maps the input \mathbf{x} into feature space, $f_C : \mathbb{R}^d \rightarrow \mathbb{R}^M$ is the concept projection layer that projects the image feature into concept activation vector, and $f_F : \mathbb{R}^M \rightarrow \mathbb{R}^{N_y}$ is the final linear classifier W_F maps the concept activation into a final prediction.

CLIP-CBM. Vanilla CBM requires labor-intensive concept activation annotations to supervise the learning of concept activation. Contrastively, as illustrated in the blue part of Fig. 3, recent CLIP-based CBMs [21, 41, 42] employ the pre-trained CLIP model to extract the image embeddings $E_I(x)$ and concept embeddings $E_T(c)$, respectively. Subsequently, CLIP-CBM obtains the concept activations \mathbf{a} by computing the similarity between image and concept embeddings, formulated as:

$$a_i = \text{sim}(E_I(x), E_T(c_i)), \quad (6)$$

$$\mathbf{a} = [a_1, a_2, \dots, a_M], \quad (7)$$

where sim indicates the cosine similarity.

The objective of CLIP-CBM is:

$$\mathcal{L}_{\text{CE}}(\hat{y}, y) = \mathbb{E}_{(x,y) \sim \mathcal{D}_{train}} [\mathcal{L}(W_F \cdot \mathbf{a}, y)], \quad (8)$$

where $\mathcal{L}_{\text{CE}}(\hat{y}, y)$ is the cross-entropy loss.

4.2. Domain Descriptors Orthogonality Loss

As mentioned in Sec. 1, CLIP-CBMs suffer from the OOD generalization problem due to the negative impact of domain-specific concepts. To erase the negative influence of domain-specific concepts, we encourage the learnable class-concept correlation matrix (*i.e.* the weight of the final linear classification layer), to be orthogonal to the language-guided synthesized domain-specific concept activations.

Following previous works [15, 25], we decompose the concept activation \mathbf{a} into two components, the *domain-specific* concept activation vector \mathbf{a}_{sp} and the *domain-shared* concept vector \mathbf{a}_{sh} , represented as:

$$\mathbf{a} = \mathbf{a}_{sp} + \mathbf{a}_{sh}, \quad (9)$$

Our goal is to erase the impact of domain-specific concepts to the final predictions, formulated as:

$$W_F \cdot \mathbf{a}_{sp} = 0. \quad (10)$$

Based on the observations in Sec. 3, we can simulate the \mathbf{a}_{sp} via computing the similarity between language-guided domain shifts and the concepts. Specifically, the language-guided class-level domain shifts Δt_{py} are the subtraction between text embeddings of prompts of possible unseen domains and the training domain (*e.g.* ‘‘A sketch of an apple’’ - ‘‘A photo of an apple’’).

$$\Delta t(p_i, y) = E_T([p_i, y]) - E_T([p_{train}, y]), \quad (11)$$

$$\mathbf{a}_{sp}(p_i, y) = \widehat{E_T(c)} \cdot \Delta t(p_i, y) \quad (12)$$

where $\widehat{E_T(c)}$ is simulated domain-specific concept activation and p_i, p_{train}, y are the unseen domain descriptor, training domain descriptor and class, respectively.

For all possible unseen domains \mathcal{P} and candidate classes \mathcal{Y} , based on Eq. (10) and Eq. (12), we derive our proposed domain descriptor orthogonality (DDO) loss:

$$\mathcal{L}_{\text{DDO}} = \mathbb{E}_{(p_i, y) \sim \mathcal{P} \times \mathcal{Y}} \left[\left\| W_F \cdot \widehat{\mathbf{a}_{sp}}(p_i, y) \right\|^2 \right] \quad (13)$$

The forward process of DDO is illustrated in the yellow part of Fig. 3. Note that the input to the DDO loss is independent of the current samples and only acts as a regularization term applied to the W_F . Therefore, it can be plugged into various CBMs. The final loss is the combination of classification loss and DDO loss, stated as:

$$\mathcal{L} = \mathcal{L}_{\text{CE}} + \lambda \mathcal{L}_{\text{DDO}} \quad (14)$$

4.3. Generate Domain Descriptors

To simulate various unseen visual domains as much as possible, we need to write numerous domain descriptors. However, hand-writing these domain descriptors can be costly, and does not scale to large numbers of unseen domains. We can automatically construct this domain descriptor set $\mathcal{P} = \{p_i\}_{i=1}^{N_p}$ by prompting a large language model, such as GPT-3.5 [22], to list possible unseen visual domains excepts for the training domain. We prompt the large language model with the input:

Q: Please list visual domains in short phrases as much as possible.

A: Here are some visual domains in short phrases: real-world photography, clipart illustrations, 3D renders...

The generated N_p domain descriptors comprise the domain descriptor set \mathcal{P} . The full generation list and further implementation details can be found in the Appendix C.

Model	Concept	Method	CUB-Painting		AwA2-clipart		LADA-Sculpture		LADV-3D	
			ID	OOD	ID	OOD	ID	OOD	ID	OOD
CLIP ZS [26]	✗	✗	62.21	52.77	95.70	90.26	91.26	82.05	71.82	66.29
CLIP LP [26]			82.00	61.40	97.11	86.75	96.81	74.40	93.68	63.81
CLIP-CBM	human	baseline	78.51	50.54	95.69	81.91	96.66	70.44	92.21	60.64
		+DDO	78.70	55.53	95.71	83.72	96.77	75.76	92.59	63.51
PCBM† [42]	ConceptNet	baseline	75.85	54.41	97.17	84.77	97.60	76.69	94.71	65.88
		+DDO	76.48	57.50	97.19	86.58	97.64	79.74	94.82	68.33
LaBO‡ [41]	LLM	baseline	81.91	56.24	97.14	84.15	97.41	74.56	99.90	63.17
		+DDO	82.34	59.60	97.26	87.66	98.12	80.00	99.93	68.01

Table 1. Performance on four single unseen domain benchmarks. For comparison, we list the performance of prevailing CBMs as baselines and report the results of integrating our proposed DDO regularizer into these baselines. † indicates re-implemented with CLIP backbone. ‡ means visual concepts are obtained with our re-implemented LLM prompts. ID is the performance on photo domains, and OOD is the generalization performance on other domains.

5. Experiments

5.1. Datasets and Baselines

We conduct experiments on seven domain adaptation benchmarks. Notably, CUB-Painting, PACS, OfficeHome and DomainNet are the previous common benchmarks, while AwA2-clipart, LADA-Sculpture, and LADV-3D are newly proposed in the paper.

Single unseen domain benchmarks. There are some classical image classification datasets with attribute annotations, which are widely applied for the evaluation of concept-based models. For instance, *CUB-Painting* is a fine-grained bird classification dataset that consists of two visual domains, the photo domain [32] and the painting domain [35]. Each image has an attribute annotation vector. Following CUB-Painting, we collect images with various other styles for photographic images from Animals with Attributes 2 (AwA2) [39], LAD-animal [47] and LAD-vehicle [47]. Specifically, we introduce three new benchmarks, namely *AwA2-clipart*, *LADA-Sculpture* and *LADV-3D*, which focused on photo→clipart, real→sculpture and real→3D model, respectively.

Multiple unseen domain benchmarks. There are also some classical domain adaptation benchmarks with multiple visual domains. *PACS* [13] is a domain adaptation benchmark with 7 classes and 4 visual styles, including art, cartoon, photo, and sketch. *OfficeHome* [31] contains 4 domains, *i.e.* art, clipart, product, realworld, where each domain consists of 65 categories. *DomainNet* [24] is a domain adaptation dataset containing 345 common classes from six visual domains, *i.e.* real, clipart, infograph, painting, quick-draw, and sketch. Following previous single domain generalization approaches [19, 48], we train on one source domain and evaluate on the other target domains. For each source domain, we report the average generalization accuracy on all target domains.

Baselines. We compare our proposed method with the following baseline approaches. 1) Black-box classifier: *CLIP-ZS* [26] uses cosine similarity between class textual representation and image representation in CLIP shared space. *CLIP-LP* [26] fits a linear classifier on top of the frozen CLIP image encoder. 2) CLIP-based CBMs: *CLIP-CBM* leverages human-written attributes to serve as a concept bank and utilizes CLIP to compute concept activation label. *PCBM* [42] uses ConceptNet [30] to retrieve concepts relevant to these classes and automatically construct the concept bank. Original PCBM employs different visual backbones on different datasets. For a fair comparison, we re-implement the PCBM with the CLIP backbone. *LaBO* [41] applies the LLM to generate abundant visual concepts in contrast to PCBM, and we employ a two-layer classifier. For each CBM baseline, we keep their original objectives to solve the optimization.

5.2. Implementation Details

We prompt GPT3.5-turbo to generate 200 domain descriptors. These domain descriptors are used across all datasets and λ is set as 1. We pre-process the domain descriptors into text embeddings by CLIP text encoder. The DDO loss is added at the final classification layer of the CBMs in a plug-in manner. Following LaBO [41], we utilize the official CLIP ViT-L/14¹ by OpenAI as the default vision backbone to extract image embeddings. We train the linear function W_F using the Adam [10] optimizer. All experiments are conducted on a single RTX3090 GPU. More implementation details and experiments with other vision backbones are listed in the Appendix C & D.

5.3. Generalization to single unseen domain

We first evaluate our model on single unseen domain benchmarks which focused on photo → others generalization.

¹<https://github.com/openai/CLIP>

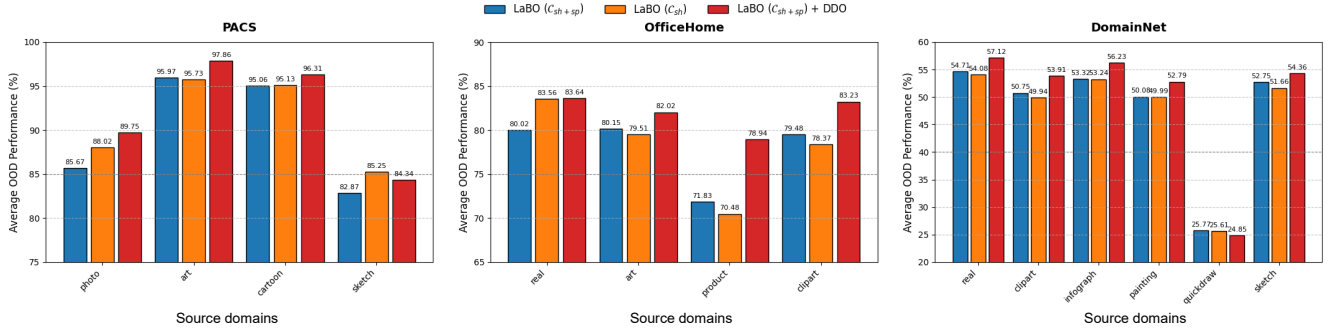


Figure 4. OOD performance on three multiple unseen domain generalization benchmarks, PACS, OfficeHome and DomainNet.

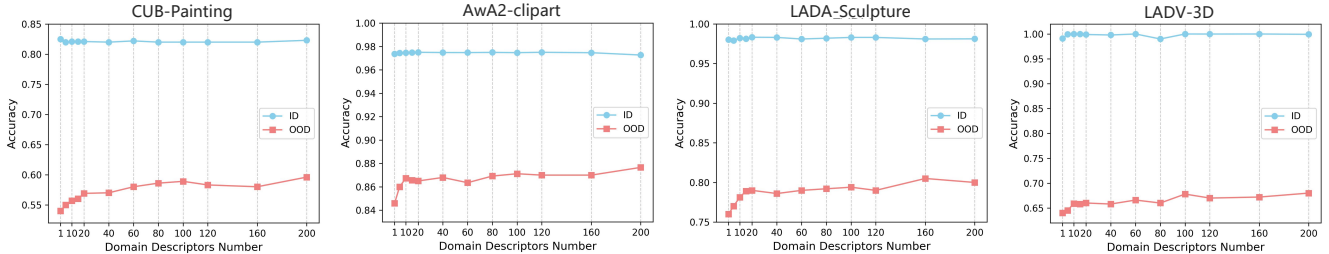


Figure 5. Ablation studies for the impact of the number of domain descriptors. For each quantity, we randomly selected domain descriptors from a total of 200 domain descriptors and averaged the results over five random selections. Results of DomainNet are shown in the Appendix D.

Table 1 shows in-distribution (ID) and out-of-distribution (OOD) accuracy on CUB-Painting, AWA2-clipart, LADA-Sculpture and LADV-3D. For all benchmarks, DDO loss is able to preserve or slightly improve the ID accuracy of each CBM while significantly improving their OOD accuracy (average 3 points improvements). We attribute the slight improvements in ID performance to the minor distribution differences between the training and test sets, even in the same visual domain. Moreover, LaBo with DDO loss can achieve competitive and superior performance on both ID and OOD performance with black-box CLIP-LP and narrow the gap with CLIP-ZS on OOD accuracy. These results demonstrate that our proposed LanCE design can effectively improve the generalization capabilities without sacrificing interpretability or classification accuracy. Besides, we notice that all models’ generalization performance to sculpture and 3D model images on the LADA-Sculpture and LADV-3D benchmark is limited, indicating generalization from 2D to 3D remains challenging.

5.4. Generalization to multiple unseen domains

To assess the ability to generalize to multiple unseen domains and the generalization capability when different domains act as the source domain, we conduct experiments on PACS, OfficeHome, and DomainNet.

Comparison with only using domain-shared concepts. In the absence of a pre-defined human-written concept

Model	Method	CUB-P	AwA2-c	LADA-S	LADV-3D
LanCE	baseline	56.24	84.15	74.56	63.17
	+DDO(IR)	57.60	85.50	77.70	65.46
	+DDO	59.60	87.66	80.00	68.01

Table 2. Ablation studies for the effect of relevance of the domain descriptors. +DDO(IR) only use the domain-irrelevant descriptors while +DDO use all domain descriptors.

set, we employ LLM to generate a concept set \mathcal{C}_{sp+in} for each dataset following LaBo [41]. This set contains both domain-specific concepts and domain-shared concepts. The main motivation of this paper is to mitigate the negative impact of domain-specific concepts. A natural question that arises is why not simply query the LLM to generate only domain-shared concepts. To explore the differences between this domain-shared approach and our DDO loss, we introduce an additional baseline, where the LLM is queried exclusively to generate a domain-shared concept set \mathcal{C}_{sh} . Specifically, we adopt the single-domain generalization evaluation setting where one source domain is used for training, and the OOD performance is averaged across other domains. As shown in Fig. 4, only using \mathcal{C}_{sh} performs well only in certain cases, such as when the source domains in the PACS dataset are photo or sketch. We attribute this to the fact that the manifestation of domain-shared concepts varies across different domains. For instance, deer antlers in photo (realistic) and cartoon (simplified or exaggerated)

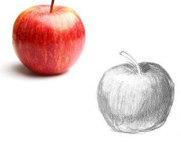
Clipart	Photo	rain 	baseline <ul style="list-style-type: none"> ● Water beads on plant tips ● Circular droplets on glass ● Wet texture on asphalt ● Radial droplet bursts ● Leaf covered in droplets 	LanCE <ul style="list-style-type: none"> ● Blurred lines for swift movement ● Oval magnifying drops ● Overlapping circle clusters ● Reflective damp surfaces ● Sharp lines with blurred edges
		Sketch	Photo	apple 
3D	Photo			airship 
		Sculpture	Photo	deer 

Figure 6. Qualitative examples about the top-5 concepts, ranking by their weights in the final linear layer W_F . Baseline indicates the results of the original LaBo. Domain-specific concepts are highlighted in red. More results are listed in Appendix E.

domains differ significantly. Moreover, we empirically observe that prompt-based methods are highly sensitive to the wording of human-written prompts. Different prompts lead to significant performance variations, yet they share a common limitation: none consistently improve performance across diverse source domains. In contrast, DDO is more flexible. It adaptively erases the influence of domain-specific concepts while suppressing domain-specific information in domain-shared concept activations, leading to stable improvements across a variety of source domains.

5.5. Ablation Studies

To explore the impact of domain descriptors on final performance, we conduct comprehensive ablation studies, with LaBO as the baseline. Specifically, we compare results with different numbers of domain descriptors and investigate the role of distinct domain descriptors.

The impact of the numbers of domain descriptors. We evaluate our method with regard to the number of domain descriptors N_p as shown in Fig. 5. The ID accuracy remains almost constant as the number of domain descriptors increases, while the OOD accuracy gradually improves with an increasing number of domain descriptors, though with diminishing returns. Specifically, when the number of domain descriptors is below 20, each additional descriptor noticeably enhances OOD accuracy. However, as the number of domain descriptors continues to increase beyond this point, the improvement in OOD accuracy slows progressively. The results shows that 100 domain descriptors are enough to achieve decent performance.

The impact of the relevance of domain descriptors. To investigate which parts of 200 domain descriptors contribute the most to OOD accuracy improvements, we manually split all domain descriptors into two components, domain-relevant descriptors and domain-irrelevant descriptors based on their relevance with the test unseen domains. For example, for the LADA-Sculpture dataset, domain-relevant domain descriptors are “sculpture”, “statue”, and

“furniture”, referring to the generated word cloud mentioned in Fig. 2 and domain-irrelevant parts are the remaining ones. Detailed splits for each dataset are listed in the Appendix D. Results are shown in the Table. 2. DDO(IR) indicates that we only use the domain-irrelevant domain descriptors to compute the DDO loss. This evaluation shows that domain-irrelevant domain descriptors can also slightly prompt the OOD accuracy on the unseen domains, although relatively fewer than the domain-relevant counterparts. It indicates those domain descriptors are not fully orthonormal, also demonstrating that the DDO loss has the potential to generalize to pure unseen visual domains that are not mentioned in the domain descriptors set \mathcal{P} .

5.6. Qualitative Results

To evaluate the effectiveness of our proposed LanCE method, we further visualize the Top-5 concepts highly related to randomly selected classes within different unseen domains as illustrated in Fig. 11. The qualitative results demonstrate that our proposed method can significantly decrease the association between the final prediction and the domain-specific concepts, in other words, erasing the impact of domain-specific concepts on the final output. More qualitative results are shown in the Appendix E.

6. Conclusion

In this paper, we propose a language-guided concept-erasing (LanCE) framework that can effectively mitigate the biased association between domain-specific concepts and the final output. We first empirically demonstrate that the pre-trained CLIP can interpret the visual domain shifts into language. And these language-guided domain shifts can distinguish the domain-specific concepts via similarity within the CLIP embedding space. Based on these observations, we introduce a plug-in domain descriptor orthogonality (DDO) loss to erase the negative impact of domain-specific concepts, and that can significantly improve the

generalization capabilities of prevailing concept bottleneck models (CBMs). We prompt the large language models (LLMs) to generate a bunch of domain descriptors to simulate numerous possible unseen domains. Moreover, considering that the current domain generalization community focuses more on generalizing to artistic unseen domains, we collect three new benchmarks that includes more difficult scenarios, *i.e.* 2D→3D, real animals→sculptures. Extensive experiments demonstrate the efficacy of our LanCE.

7. Acknowledgement

This work was supported in part by the National Natural Science Foundation of China under Grant U21B2006; in part by Shaanxi Youth Innovation Team Project; in part by the Fundamental Research Funds for the Central Universities QTZX24003 and QTZX22160; in part by the 111 Project under Grant B18039; Hao Zhang acknowledges the support of NSFC (62301384); Excellent Young Scientists Fund (Overseas); Foundation of National Key Laboratory of Radar Signal Processing under Grant JKW202308. Zhengjue Wang acknowledges the support of NSFC (62301407).

References

- [1] Jin Chen, Zhi Gao, Xinxiao Wu, and Jiebo Luo. Meta-causal learning for single domain generalization. In *Proceedings of the IEEE/CVF Conference on Computer Vision and Pattern Recognition*, pages 7683–7692, 2023. 2
- [2] Lisa Dunlap, Clara Mohri, Devin Guillory, Han Zhang, Trevor Darrell, Joseph E Gonzalez, Aditi Raghunathan, and Anna Rohrbach. Using language to extend to unseen domains. *International Conference on Learning Representations (ICLR)*, 2023. 3, 12
- [3] Lisa Dunlap, Alyssa Umino, Han Zhang, Jiezhi Yang, Joseph E Gonzalez, and Trevor Darrell. Diversify your vision datasets with automatic diffusion-based augmentation. *Advances in neural information processing systems*, 36:79024–79034, 2023. 2, 3
- [4] Abolfazl Farahani, Sahar Voghoei, Khaled Rasheed, and Hamid R Arabnia. A brief review of domain adaptation. *Advances in data science and information engineering: proceedings from ICDATA 2020 and IKE 2020*, pages 877–894, 2021. 3
- [5] Kaiming He, Haoqi Fan, Yuxin Wu, Saining Xie, and Ross Girshick. Momentum contrast for unsupervised visual representation learning. In *Proceedings of the IEEE/CVF conference on computer vision and pattern recognition*, pages 9729–9738, 2020. 3
- [6] Kaiming He, Xinlei Chen, Saining Xie, Yanghao Li, Piotr Dollár, and Ross Girshick. Masked autoencoders are scalable vision learners. In *Proceedings of the IEEE/CVF conference on computer vision and pattern recognition*, pages 16000–16009, 2022. 3
- [7] Amir Hertz, Ron Mokady, Jay Tenenbaum, Kfir Aberman, Yael Pritch, and Daniel Cohen-Or. Prompt-to-prompt image editing with cross attention control. *arXiv preprint arXiv:2208.01626*, 2022. 3
- [8] Chao Jia, Yinfei Yang, Ye Xia, Yi-Ting Chen, Zarana Parekh, Hieu Pham, Quoc Le, Yun-Hsuan Sung, Zhen Li, and Tom Duerig. Scaling up visual and vision-language representation learning with noisy text supervision. In *International conference on machine learning*, pages 4904–4916. PMLR, 2021. 1
- [9] Been Kim, Martin Wattenberg, Justin Gilmer, Carrie Cai, James Wexler, Fernanda Viegas, et al. Interpretability beyond feature attribution: Quantitative testing with concept activation vectors (tcav). In *International conference on machine learning*, pages 2668–2677. PMLR, 2018. 2
- [10] Diederik P Kingma. Adam: A method for stochastic optimization. *arXiv preprint arXiv:1412.6980*, 2014. 6
- [11] Pang Wei Koh, Thao Nguyen, Yew Siang Tang, Stephen Mussmann, Emma Pierson, Been Kim, and Percy Liang. Concept bottleneck models. In *International conference on machine learning*, pages 5338–5348. PMLR, 2020. 1, 2, 5
- [12] Gihyun Kwon and Jong Chul Ye. Clipstyler: Image style transfer with a single text condition. In *Proceedings of the IEEE/CVF Conference on Computer Vision and Pattern Recognition*, pages 18062–18071, 2022. 3
- [13] Da Li, Yongxin Yang, Yi-Zhe Song, and Timothy M Hospedales. Deeper, broader and artier domain generalization. In *Proceedings of the IEEE international conference on computer vision*, pages 5542–5550, 2017. 2, 6
- [14] Jichang Li, Guanbin Li, Yemin Shi, and Yizhou Yu. Cross-domain adaptive clustering for semi-supervised domain adaptation. In *Proceedings of the IEEE/CVF conference on computer vision and pattern recognition*, pages 2505–2514, 2021. 3
- [15] Ya Li, Xinmei Tian, Mingming Gong, Yajing Liu, Tongliang Liu, Kun Zhang, and Dacheng Tao. Deep domain generalization via conditional invariant adversarial networks. In *Proceedings of the European conference on computer vision (ECCV)*, pages 624–639, 2018. 5
- [16] Huaishao Luo, Lei Ji, Ming Zhong, Yang Chen, Wen Lei, Nan Duan, and Tianrui Li. Clip4clip: An empirical study of clip for end to end video clip retrieval. *arXiv preprint arXiv:2104.08860*, 2021. 3
- [17] Jiawei Ma, Po-Yao Huang, Saining Xie, Shang-Wen Li, Luke Zettlemoyer, Shih-Fu Chang, Wen-Tau Yih, and Hu Xu. Mode: Clip data experts via clustering. In *Proceedings of the IEEE/CVF Conference on Computer Vision and Pattern Recognition*, pages 26354–26363, 2024. 3
- [18] Jiawei Ma, Yulei Niu, Shiyuan Huang, Guangxing Han, and Shih-Fu Chang. Widin: Wording image for domain-invariant representation in single-source domain generalization. *arXiv preprint arXiv:2405.18405*, 2024. 3
- [19] Lianbo Ma, Haidong Kang, Guo Yu, Qing Li, and Qiang He. Single-domain generalized predictor for neural architecture search system. *IEEE Transactions on Computers*, 2024. 3, 6
- [20] Saeid Motiian, Marco Piccirilli, Donald A Adjeroh, and Gianfranco Doretto. Unified deep supervised domain adaptation and generalization. In *Proceedings of the IEEE international conference on computer vision*, pages 5715–5725, 2017. 3

- [21] Tuomas Oikarinen, Subhro Das, Lam M Nguyen, and Tsui-Wei Weng. Label-free concept bottleneck models. *arXiv preprint arXiv:2304.06129*, 2023. 2, 5
- [22] OpenAI. Chatgpt. <https://www.openai.com/chatgpt>, 2023. 5
- [23] Or Patashnik, Zongze Wu, Eli Shechtman, Daniel Cohen-Or, and Dani Lischinski. Styleclip: Text-driven manipulation of stylegan imagery. In *Proceedings of the IEEE/CVF international conference on computer vision*, pages 2085–2094, 2021. 3
- [24] Xingchao Peng, Qinxun Bai, Xide Xia, Zijun Huang, Kate Saenko, and Bo Wang. Moment matching for multi-source domain adaptation. In *Proceedings of the IEEE International Conference on Computer Vision*, pages 1406–1415, 2019. 2, 6
- [25] Vihari Piratla, Praneeth Netrapalli, and Sunita Sarawagi. Efficient domain generalization via common-specific low-rank decomposition. In *International conference on machine learning*, pages 7728–7738. PMLR, 2020. 3, 5
- [26] Alec Radford, Jong Wook Kim, Chris Hallacy, Aditya Ramesh, Gabriel Goh, Sandhini Agarwal, Girish Sastry, Amanda Askell, Pamela Mishkin, Jack Clark, et al. Learning transferable visual models from natural language supervision. In *International conference on machine learning*, pages 8748–8763. PMLR, 2021. 1, 3, 6, 15
- [27] Gesina Schwalbe. Concept embedding analysis: A review. *arXiv preprint arXiv:2203.13909*, 2022. 1
- [28] Chenming Shang, Shiji Zhou, Hengyuan Zhang, Xinzhe Ni, Yujiu Yang, and Yuwang Wang. Incremental residual concept bottleneck models. In *Proceedings of the IEEE/CVF Conference on Computer Vision and Pattern Recognition*, pages 11030–11040, 2024. 2
- [29] Sheng Shen, Liunian Harold Li, Hao Tan, Mohit Bansal, Anna Rohrbach, Kai-Wei Chang, Zhewei Yao, and Kurt Keutzer. How much can clip benefit vision-and-language tasks? *arXiv preprint arXiv:2107.06383*, 2021. 3
- [30] Robyn Speer, Joshua Chin, and Catherine Havasi. Conceptnet 5.5: An open multilingual graph of general knowledge. In *Proceedings of the AAAI conference on artificial intelligence*, 2017. 6
- [31] Hemanth Venkateswara, Jose Eusebio, Shayok Chakraborty, and Sethuraman Panchanathan. Deep hashing network for unsupervised domain adaptation. In *Proceedings of the IEEE conference on computer vision and pattern recognition*, pages 5018–5027, 2017. 2, 6
- [32] Catherine Wah, Steve Branson, Peter Welinder, Pietro Perona, and Serge Belongie. The caltech-ucsd birds-200-2011 dataset. 2011. 6
- [33] Jindong Wang, Cuiling Lan, Chang Liu, Yidong Ouyang, Tao Qin, Wang Lu, Yiqiang Chen, Wenjun Zeng, and S Yu Philip. Generalizing to unseen domains: A survey on domain generalization. *IEEE transactions on knowledge and data engineering*, 35(8):8052–8072, 2022. 3
- [34] Jindong Wang, Cuiling Lan, Chang Liu, Yidong Ouyang, Tao Qin, Wang Lu, Yiqiang Chen, Wenjun Zeng, and S Yu Philip. Generalizing to unseen domains: A survey on domain generalization. *IEEE transactions on knowledge and data engineering*, 35(8):8052–8072, 2022. 2, 3
- [35] Sinan Wang, Xinyang Chen, Yunbo Wang, Mingsheng Long, and Jianmin Wang. Progressive adversarial networks for fine-grained domain adaptation. In *Proceedings of the IEEE/CVF conference on computer vision and pattern recognition*, pages 9213–9222, 2020. 2, 6
- [36] Zijian Wang, Yadan Luo, Ruihong Qiu, Zi Huang, and Mahsa Baktashmotlagh. Learning to diversify for single domain generalization. In *Proceedings of the IEEE/CVF International Conference on Computer Vision*, pages 834–843, 2021. 3
- [37] Zhizhong Wang, Lei Zhao, and Wei Xing. Stylediffusion: Controllable disentangled style transfer via diffusion models. In *Proceedings of the IEEE/CVF International Conference on Computer Vision*, pages 7677–7689, 2023. 3
- [38] Tiansheng Wen, Yifei Wang, Zequn Zeng, Zhong Peng, Yudi Su, Xinyang Liu, Bo Chen, Hongwei Liu, Stefanie Jegelka, and Chenyu You. Beyond matryoshka: Revisiting sparse coding for adaptive representation. *arXiv preprint arXiv:2503.01776*, 2025. 3
- [39] Yongqin Xian, Christoph H Lampert, Bernt Schiele, and Zeynep Akata. Zero-shot learning—a comprehensive evaluation of the good, the bad and the ugly. *IEEE transactions on pattern analysis and machine intelligence*, 41(9):2251–2265, 2018. 2, 6, 12
- [40] Tongkun Xu, Weihua Chen, Pichao Wang, Fan Wang, Hao Li, and Rong Jin. Cdtrans: Cross-domain transformer for unsupervised domain adaptation. *arXiv preprint arXiv:2109.06165*, 2021. 3
- [41] Yue Yang, Artemis Panagopoulou, Shenghao Zhou, Daniel Jin, Chris Callison-Burch, and Mark Yatskar. Language in a bottle: Language model guided concept bottlenecks for interpretable image classification. In *Proceedings of the IEEE/CVF Conference on Computer Vision and Pattern Recognition*, pages 19187–19197, 2023. 1, 2, 5, 6, 7, 15
- [42] Mert Yuksekgonul, Maggie Wang, and James Zou. Post-hoc concept bottleneck models. *arXiv preprint arXiv:2205.15480*, 2022. 1, 2, 5, 6, 15
- [43] Yuan Zang, Tian Yun, Hao Tan, Trung Bui, and Chen Sun. Pre-trained vision-language models learn discoverable visual concepts. *arXiv preprint arXiv:2404.12652*, 2024. 2
- [44] Zequn Zeng, Hao Zhang, Ruiying Lu, Dongsheng Wang, Bo Chen, and Zhengjue Wang. Conzic: Controllable zero-shot image captioning by sampling-based polishing. In *Proceedings of the IEEE/CVF Conference on Computer Vision and Pattern Recognition*, pages 23465–23476, 2023. 3, 12
- [45] Zequn Zeng, Jianqiao Sun, Hao Zhang, Tiansheng Wen, Yudi Su, Yan Xie, Zhengjue Wang, and Bo Chen. Hicscore: A hierarchical metric for image captioning evaluation. *arXiv preprint arXiv:2407.18589*, 2024. 3
- [46] Zequn Zeng, Yan Xie, Hao Zhang, Chiyu Chen, Bo Chen, and Zhengjue Wang. Meacap: Memory-augmented zero-shot image captioning. In *Proceedings of the IEEE/CVF Conference on Computer Vision and Pattern Recognition*, pages 14100–14110, 2024. 3
- [47] Bo Zhao, Yanwei Fu, Rui Liang, Jiahong Wu, Yonggang Wang, and Yizhou Wang. A large-scale attribute dataset for zero-shot learning. In *Proceedings of the IEEE/CVF confer-*

- ence on computer vision and pattern recognition workshops*, pages 0–0, 2019. [2](#), [6](#)
- [48] Guangtao Zheng, Mengdi Huai, and Aidong Zhang. Advst: Revisiting data augmentations for single domain generalization. In *Proceedings of the AAAI conference on artificial intelligence*, pages 21832–21840, 2024. [3](#), [6](#)
- [49] Kaiyang Zhou, Ziwei Liu, Yu Qiao, Tao Xiang, and Chen Change Loy. Domain generalization: A survey. *IEEE Transactions on Pattern Analysis and Machine Intelligence*, 45(4):4396–4415, 2022. [2](#), [3](#)

A. New Datasets

Dataset Statistics. We collect three new domain adaptation datasets, *i.e.* AwA2-clipart, LADA-Sculpture, and LADV-3D based on previous attribute-annotated datasets [2, 39] in this paper. Table. 3 are some basic dataset statistics. Fig. 7 has shown some samples from each dataset. To visualize the domain shifts in these three new datasets, we use CLIP ViT-L/14 to extract image features for images in these datasets and use the TSNE tools to visualize all image features.

Dataset Statistics	AwA2-clipart	LADA-Sculpture	LADV-3D
Data field	animals	animals	vehicles
Visual domains	photo,clipart	real,sculpture	real, 3d renders
Number of images	37328,5319	13240,2162	17080,3587
Number of categories	50	50	50

Table 3. Some dataset statistics of AwA2-clipart, LADA-Sculpture, LADV-3D.

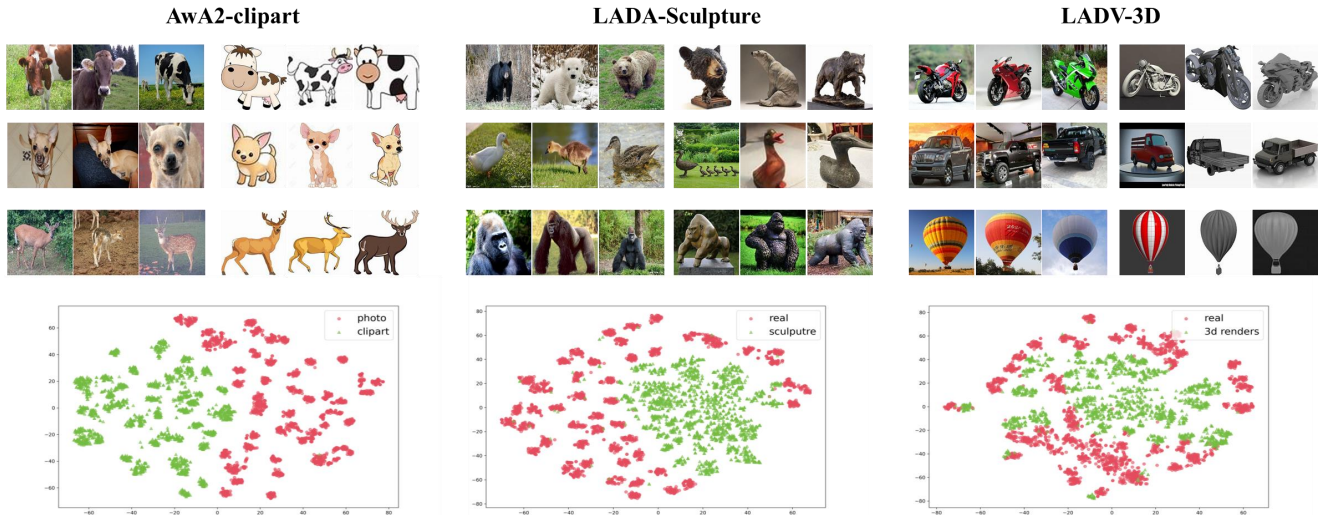


Figure 7. Some randomly selected samples and CLIP feature TSNE visualization of all samples on our proposed three benchmarks.

B. Empirical studies

This paper’s key insights are derived from our empirical studies that the VLMs can interpret the visual domain shifts into language, in other words, visual domain shifts and descriptions of different domains are consistent in the VLM embedding space. The main paper lists the results between two unseen visual domains (*i.e.* “sketch” and “sculpture”) and the training domain (“photo”). In this section, we list more results between unseen visual domains like “clipart”, “3d model” and “painting” in Fig. 8. Similar to the main paper, the class-level descriptors generated by ConZIC [44] describe the visual difference. The style descriptions for the common photo domain (subtrahend) are generally implicit in the training caption corpus, thus, the class-level descriptors prominently consist of style descriptions about the unseen visual domains (minuend). To better visualize the global semantic direction, we aggregate all class-level descriptors into a final word cloud format, where prominent words represent the main visual direction between the two visual domains. For instance, semantical words “cartoon, view, character, draw, illustration” indicate the main style direction of the “clipart” domain. This demonstrates that the visual domain shifts can be approximated by some domain-related style descriptors, while these style descriptors can be used to compute class-level textual domain differences.

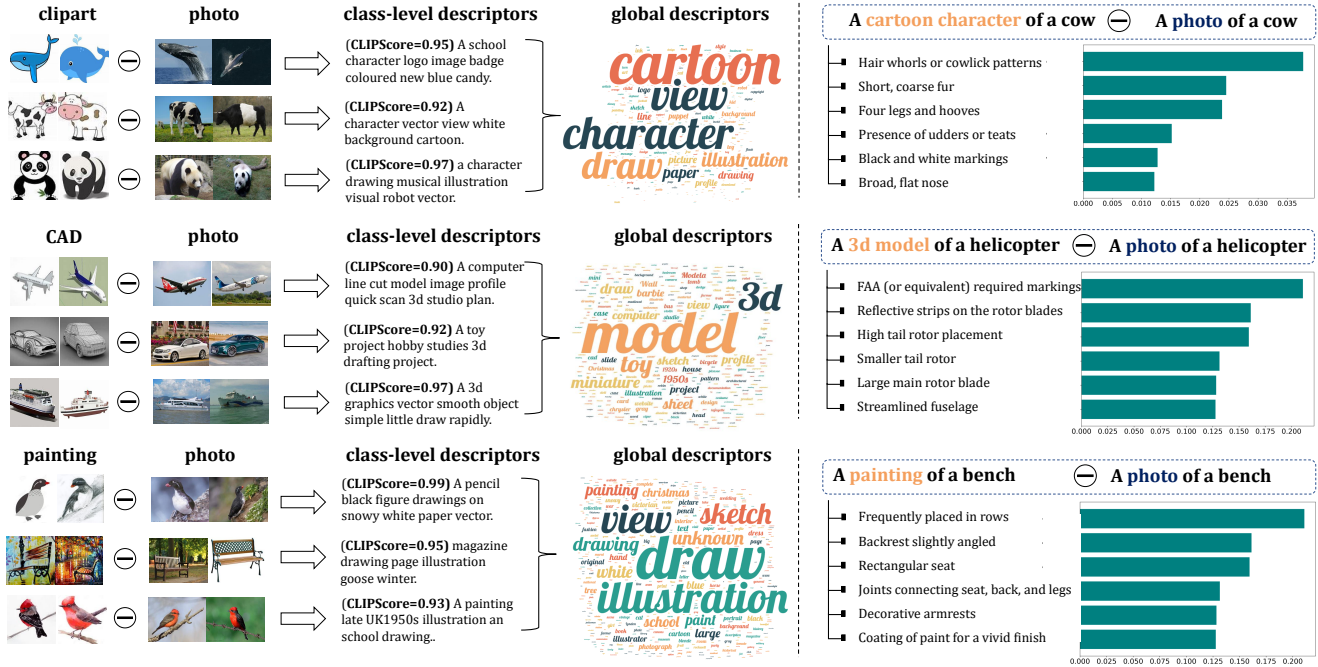
Then, we can utilize these textual domain differences to discover the domain-specific concepts. Concretely, we can concatenate these domain descriptors with specific classes in a prompt style, such as “A cartoon character of a cow”, denoted as t_{tgt} . Similarly, we can construct a prompt for photo domains like “A photo of a cow”, denoted as t_{src} . For each discriminative

visual concept c_i , we can compute the similarity s_i with this class-level textual domain shifts in the CLIP embedding space, as:

$$\Delta t = E_T(t_{tgt}) - E_T(t_{src}) \quad (15)$$

$$s_i = E_T(c_i) \cdot \Delta t, \quad (16)$$

where E_T means CLIP text encoder. Finally, we can get all concept activation $\{s_i\}_{i=1}^M$. We empirically find that those concepts with higher similarity are often domain-specific concepts that exhibit substantial variation between two domains. Therefore, $S = [s_1, \dots, s_M]$ can be viewed as a domain-specific concept activation a_{sp} . These observations provide the key insights of this paper.



(a) Interpret the visual domain shifts into language.

(b) Discover the domain-specific concepts.

Figure 8. Empirical studies on more domain shifts.

C. More implementation details of DDO loss

In this section, we will introduce more implementation details about our proposed LanCE framework.

C.1. Generating domain descriptors

Based on the empirical observations in Sec. B, we aim to achieve generalization across a wide range of unseen visual domains by leveraging a large language model (LLM) to generate domain descriptors \mathcal{P} . A detailed list is shown in Fig. 9.

C.2. Textual domain shifts embeddings

After we get all domain descriptors $\mathcal{P} = \{p_i\}_{i=1}^{N_p}$, we can use these domain descriptors to compute textual domain shift embeddings based on Eq. (15). Specifically, we set the training domain as “photo” and compute the difference between two domain-related class prompts. Finally, we can get all class-level textual domain shifts $[\Delta t(p_i, y)]_{N_p \times N_y}$.

C.3. Details of DDO loss

DDO aims to encourage the orthogonality between all domain-specific concept activations $[a_{sp}(p_i, y)]_{N_p \times N_y}$ and class prototype concept activations (*i.e.* linear weight W_F). The computation of $a_{sp}(p_i, y)$ as:

$$a_{sp}(p_i, y) = [\Delta t(p_i, y) \cdot E_T(c_1), \dots, \Delta t(p_i, y) \cdot E_T(c_M)] \quad (17)$$

- **Concept prompt:** *What are useful visual features for identifying an {classname}. You can consider visual features from appearance, color, pattern, shape perspectives. please describe at least 50 visual features without class name in sentence list: [].*
- **Domain Descriptor Prompt:** *Generate 200 new domain description prompts modeled on "a photo of a {}"*

Answered Domain descriptors (processed): [painting, clipart, infographic, quickdraw, sketch, cartoon character, advertising posters, sculpture, watercolor, 3D model, blueprint, silhouette, vintage photo, digital art, pencil drawing, technical illustration, doodle, woodcut, lithograph, oil painting, gouache painting, embroidery, charcoal sketch, etching, tattoo design, comic strip, collage, pop art, manga style drawing, minimalist drawing, pixel art, sepia photo, retro style, low-poly model, fantasy art, surrealist painting, futuristic concept art, impressionist painting, hyperrealistic drawing, chalkboard sketch, photo collage, CGI render, stained glass, anime style, Renaissance painting, Victorian engraving, children’s book illustration, pen and ink drawing, crayon drawing, blueprint diagram, steampunk version, street art mural, pastel drawing, scientific diagram, psychedelic art, editorial cartoon, pointillism painting, decorative ornament, folk art version, holographic image, VR model, bronze statue, ancient cave painting, sci-fi style, children coloring book, mixed media art, conceptual sketch, steampunk mechanical drawing, hand-painted mural, pastel artwork, illustrated diagram, vector graphic, medieval manuscript, baroque painting, Cubist painting, Art Deco version, Art Nouveau illustration, acrylic painting, neon sign, icon design, shadow silhouette, cut-paper art, tapestry, cross-stitch pattern, visual novel character, emoji, logo, banner, motion graphic, kinetic sculpture, vintage postcard, LED display, glass sculpture, sand art representation, flower arrangement, fabric pattern, Egyptian hieroglyph, 16-bit video game character, pottery design, metal engraving, origami model, cyberpunk illustration, graffiti stencil, stained glass panel, Rorschach inkblot, Gothic architecture detail, postage stamp, wireframe model, LEGO model, hologram, paper doll, bubble letter graffiti, cookie cutter shape, emoji sticker, flipbook animation, crystal carving, sand sculpture, totem pole, Moai statue, scientific model, photo negative, pop-up book, clay sculpture, fabric print, kinetic art piece, chalk pavement art, scrimshaw, augmented reality filter, laser-cut wood model, beadwork pattern, lenticular print, tarot card, astrological chart, glass mosaic, domino tile, rubber stamp, fashion illustration, tattoo flash, 2D animation cell, comic book panel, topographic map, ASCII art, street photography shot, stone carving, bookplate illustration, linocut, album cover, silhouette photo, flipbook, watercolor wash, 4-bit pixel icon, map illustration, animated GIF, 3D hologram, typography art, paper cutout, retrowave poster, constellation, steampunk icon, painted ceramic tile, abstract representation, shadow puppet, cave engraving, dot matrix print, Rube Goldberg machine, aerial view photo, album art design, topographic elevation map, needlepoint design, quilling art piece, badge design, marble statue, glass etching, logo badge, postage stamp illustration, embossed print, neon artwork, street poster, ancient rune, steampunk watch gear, environmental infographic, safety sign, blueprint schematic, wire sculpture, papercraft model, photorealistic painting, vintage label, linocut print, painting on driftwood, cave wall painting, tribal tattoo, doodle sticker, video game cover, emoji art, lava lamp pattern, comic character, floral arrangement shaped, retro poster, minimalist icon, classic movie poster, botanical illustration, cross-sectional diagram, video game avatar, medieval tapestry, carved pumpkin in the shape]

Figure 9. LLM prompts to generate visual concepts and domain descriptors and detailed generated domain descriptor list.

Model	FLOPs (in billions)	Parameters	Memory Usage (in MB)
baseline	13285.1	63224	918.0
LanCE	13287.7	63224	1038.1

Table 4. Comparison of computation complexity, including FLOPs, trainable parameters, and estimated memory usage.

Notably, the DDO loss is independent of specific input samples, as all $[\mathbf{a}_{sp}(p_i, y)]N_p \times N_y$ are processed by W_F collectively with each batch of image samples.

D. More ablation studies

Effect of CLIP backbone. Table. 5 and Table. 6 have shown the detailed results with CLIP ViT-B/32 and CLIP ViT-L/14, demonstrating that our proposed DDO regularizer can improve the OOD accuracy across different CLIP image backbones.

Effect of the numbers of domain descriptors. Fig. 10 provides the ablation studies on DomainNet. Similar to other results on other datasets, the OOD accuracy gradually improves with an increasing number of domain descriptors.

Effect of relevance of domain descriptors. Table. 7 has shown some relevant keywords about each benchmark. We remove domain descriptors containing these keywords and investigate the contribution of remaining domain-irrelevant domain descriptors to improving OOD accuracy. Fig. 8 shows the results on DomainNet.

Computation complexity. To evaluate the gained computation complexity brought by DDO loss, we list the comparison results of FLOPs, trainable parameters, and estimated memory usage. Results are shown in Table. 4, as we can see, the gained computation complexity is minor and almost negligible. It demonstrates that our proposed DDO loss is a plug-in loss that can be applied to many concept-based models without changing model architecture and increasing too much computation cost.

Model	Concept	Method	CUB-Painting		AwA2-clipart		LADA-Sculpture		LADV-3D	
			ID	OOD	ID	OOD	ID	OOD	ID	OOD
CLIP ViT-B/32										
CLIP ZS [26]	✗	✗	65.27	40.14	91.50	67.44	87.17	48.98	84.36	50.07
CLIP LP [26]			51.59	44.57	91.72	79.32	89.46	65.12	68.28	60.49
CLIP-CBM	human	baseline	61.05	35.08	92.38	62.14	94.52	48.89	87.85	53.25
		+DDO	62.88	39.51	90.95	66.29	95.05	53.70	87.29	55.42
PCBM† [42]	ConceptNet	baseline	58.31	38.83	93.41	71.78	95.31	55.64	90.11	56.87
		+DDO	58.81	39.91	92.58	69.11	95.76	57.96	90.03	57.18
LaBO [41]	LLM	baseline	67.57	35.35	93.90	62.60	96.70	77.63	99.44	56.00
		+DDO	67.83	37.28	94.50	71.70	98.27	79.69	99.13	58.88
CLIP ViT-L/14										
CLIP ZS [26]	✗	✗	62.21	52.77	95.70	90.26	91.26	82.05	71.82	66.29
CLIP LP [26]			82.00	61.40	97.11	86.75	96.81	74.40	93.68	63.81
CLIP-CBM	human	baseline	78.51	50.54	95.69	81.91	96.66	70.44	92.21	60.64
		+DDO	78.70	55.53	95.71	83.72	96.77	75.76	92.59	63.51
PCBM† [42]	ConceptNet	baseline	75.85	54.41	97.17	84.77	97.60	76.69	94.71	65.88
		+DDO	76.48	57.50	97.19	86.58	97.64	79.74	94.82	68.33
LaBO [41]	LLM	baseline	81.91	56.24	97.14	84.15	97.41	74.56	99.90	63.17
		+DDO	82.34	59.60	97.26	87.66	98.12	80.00	99.93	68.01

Table 5. Detailed accuracy performance comparison on single unseen domain benchmarks, including CUB-Painting, AwA2-clipart, LADA-Sculpture, and LADV-3D.

DomainNet.								
Model	Method	ID real	OOD					Avg
			clipart	infograph	painting	quickdraw	Sketch	
CLIP ViT-B/32								
LaBO [41]	baseline	86.11	60.60	35.00	54.64	8.40	49.7	41.67
	+DDO	86.33	64.00	39.66	58.90	8.57	52.9	44.81
CLIP ViT-L/14								
LaBO [41]	baseline	91.20	76.04	48.41	66.16	16.58	66.35	55.63
	+DDO	91.29	77.37	53.00	68.91	17.27	69.04	56.20

Table 6. Detailed accuracy performance comparison on multiple unseen domain benchmarks, *i.e.* DomainNet.

E. More qualitative results

Fig. 11 has shown more qualitative results about the top-5 visual concepts, ranked by the weights in W_F , demonstrating that our proposed DDO regularizer can reduce the correlation between domain-specific concepts and final predictions.

F. Human evaluation

To validate the efficacy of our proposed method, we conduct a human evaluation on the top 10 visual concepts that exhibit a high correlation with the final class, ranked by the weights W_F trained on DomainNet. The evaluation considers two key aspects: *Discriminability* and *Generalizability*. For each concept, we present several images from all visual domains and invite three human experts to assign a score ranging from 0 to 4. Specifically, for *Discriminability*, a score of 0 indicates the concept is unrelated to the corresponding category, while a score of 4 signifies the concept is a salient visual feature for

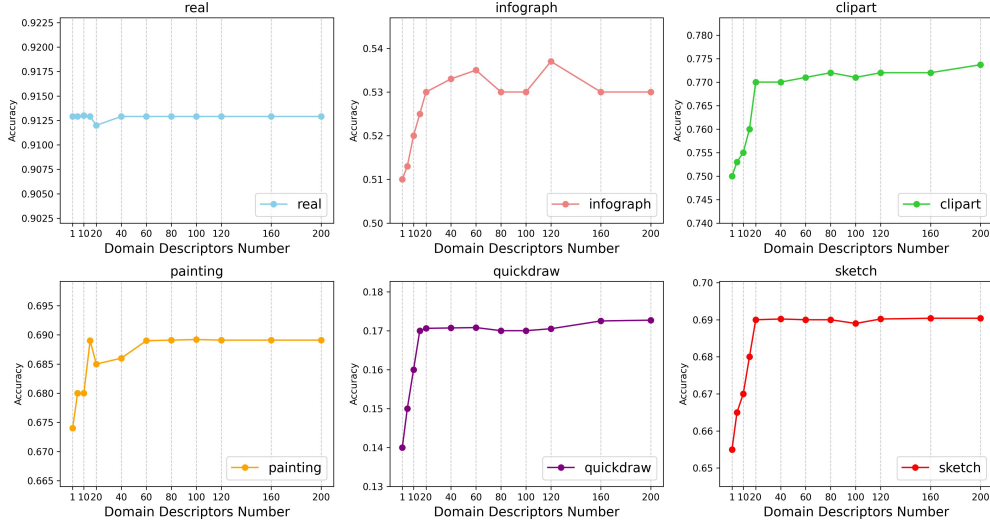


Figure 10. Ablation studies about the numbers of the domain descriptors on DomainNet.

Dataset	Relevant descriptors (keywords)
CUB-Painting	painting, sketch, watercolor, drawing, doodle, art
AwA2-clipart	clipart, cartoon, emoji, comic, anime, avatar, animated
LADA-Sculpture	sculpture, 3D, statue
LADV-3D	3D, CGI, VR, low-poly
DomainNet	painting, clipart, infographic, quickdraw, sketch, watercolor, cartoon, collage, art, drawing, sketch, illustration, doodle, poster emoji, comic, anime

Table 7. Relevant descriptors for each benchmark.

		real	clipart	painting	infograph	sketch	quickdraw
LanCE	baseline	91.20	76.04	66.16	48.41	66.35	16.58
	+DDO(IR)	91.20	76.60	67.80	50.00	67.74	16.30
	+DDO	91.29	77.37	68.91	53.0	69.04	17.27

Table 8. Ablation studies on DomainNet for the effect of relevance of the domain descriptors. +DDO(IR) only use the domain-irrelevant descriptors while +DDO use all domain descriptors.

the category. For *Generalizability*, a score of 0 indicates the concept exists only in a single domain, whereas a score of 4 represents a domain-invariant concept. The scores from the three annotators are averaged, and concepts with an average score greater than 2 are classified as either discriminative or domain-invariant concepts. For each concept, we generate a binary label based on these classifications. Finally, we analyze the percentage of discriminative and domain-invariant concepts to report the final results. To evaluate these two metrics, we select top-10 concepts for each class ranking by their weights in the

Model	Discriminability(%)	Generalizability(%)
baseline	75	64
LanCE	79	82

Table 9. Human evaluation about the percentage of distinguishing concepts and percentage of domain-invariant concepts.

final layer W_F , and ask annotators to judge whether each concept meets the demands above. The ratio of accurate concepts are shown in the Table. 9 where our proposed LanCE achieves better results than the baseline LaBo, demonstrating the effectiveness of languid-guided concept erasing design can significantly decrease the association between domain-specific concepts and the final output.

G. Limitations

Our method highly depends on pre-trained VLMs like CLIP and LLMs like GPT-3.5. However, these models are limited in application to some professional fields like medical treatments. We think further integration of an extra knowledge base and task-specific fine-tuning of these pre-trained models is a potential solution to solve these limitations. We hope this work can prompt the development of robust interpretable models.

clipart	Photo	bat		LaBO	LanCE	Painting	Photo	Baird Sparrow		LaBO	LanCE	
		<ul style="list-style-type: none"> Glossy shine on wing membranes Forearm proportion compared to wingspan Membrane texture on wings Wing translucency Long fingers within wings 	<ul style="list-style-type: none"> Clawed feet for hanging Forearm proportion compared to wingspan Membrane texture on wings Long fingers within wings Small, rodent-like body shape 	<ul style="list-style-type: none"> Bill is short and pink clump of grass found in open areas with some trees or shrubs nests in sagebrush songbird with a clear, whistled song 	<ul style="list-style-type: none"> small, brown and white sparrow brown streaked head tail is long and brown with white stripes nests in grasses or shrubs back that is brownish 							
Sculpture	Photo	rhinoceros		LaBO	LanCE	3D	Photo	airliner		LaBO	LanCE	
		<ul style="list-style-type: none"> Bushy tail Darker to lighter gradient across the leg fur Ears have tips Smooth, flowing fur texture small stature compared to other wild canids 	<ul style="list-style-type: none"> Bushy tail Ears have tips Front paws more moved forward when standing Fur displays a reddish hue Lower jaw often prominently displays canines 	<ul style="list-style-type: none"> Antennas on the fuselage top or bottom Airline-specific patterns Multiple emergency exit doors Painted stripes or bands Straight-aligned windows 	<ul style="list-style-type: none"> Antennas on the fuselage top or bottom Straight-aligned windows Vortex generators on wings Straight-aligned windows Seamless wing root integration 							
truck	photo	clipart	painting	infograph	sketch	quickdraw	photo	clipart	painting	infograph	sketch	quickdraw
<ul style="list-style-type: none"> Graphic or logo decals Heavy-duty tires Rooftop air hornsThick, wrinkled skin Textured bed liner Visible exhaust pipe on the side 	<ul style="list-style-type: none"> Boxy, angular design Massive rectangular front grille Wheel arches outlining the tires Fenders with auxiliary lights Dominant vertical bars 	<ul style="list-style-type: none"> Distinctive rustling sound from the canopy Fan palm leaves radiate from a central point Glistening foliage under strong sunlight Coconuts or fruits may be present at crown Some palms display spiny leaf stems 	<ul style="list-style-type: none"> Arching, fan-like fronds Cluster of large, radiating leaves Crown-shaped foliage atop a singular trunk Island or waterfront proximity Symmetrical leaf arrangement 									

Figure 11. More qualitative results. top-5 concepts, ranking by their weights in the final linear layer W_F . Baseline indicates the results of the original LaBo. Domain-specific concepts are highlighted in red.